Reconfigurable Intelligent Surface (RIS)-Assisted Beyond 5G(B5G) Networks

Tiancheng Chen (tic041@ucsd.edu)
Xinli Xiang (x3xiang@ucsd.edu)

I. Motivation

The rapid evolution of wireless communication technologies has led to the widespread adoption of 5G networks, which rely on advanced technologies such as millimeter wave (MMwave) and massive multiple-input multiple-output (MIMO) to achieve high transmission rates and low latency. However, these technologies face significant challenges, including limited transmission distance, uncontrollable signal channel information, signal interference, high energy consumption, and substantial hardware costs. These challenges hinder the large-scale deployment of beyond 5G (B5G) wireless networks, which are expected to support even higher data rates, greater connectivity, and more reliable communication.

Moreover, natural disasters such as earthquakes, landslides, and debris flows frequently inflict severe damage to terrestrial communication infrastructure, disrupting essential communication channels that are vital for coordinating disaster response and recovery efforts. Although satellite communication systems offer a viable alternative, they are not immune to the challenges posed by adverse weather conditions and physical obstructions caused by disasters. This underscores the necessity for innovative communication technologies that can ensure uninterrupted connectivity during emergencies, enabling timely and effective disaster management.

To address these issues, innovative solutions are required to enhance signal quality, extend transmission distance, and improve energy efficiency. Reconfigurable Intelligent Surfaces (RIS) have emerged as a promising technology to overcome these challenges by passively reflecting signals with controllable phase shifts, thereby optimizing wireless communication performance.

II. Background and Approach

Wireless communication networks have undergone significant advancements over the past three decades, with 5G networks representing the latest milestone. The use of MMwave and massive MIMO technologies has enabled 5G networks to achieve unprecedented data rates and network coverage. However, these technologies still have their limitations. MMwave signals, despite their high energy and short wavelengths, suffer from severe path loss, especially in urban environments where physical obstructions can distort or block signals. Additionally, the complexity of precoding and beamforming in massive MIMO systems increases with the number of antennas, leading to higher energy consumption and hardware costs [1]. These challenges necessitate the development of new technologies and optimization methods to ensure the successful deployment of B5G networks.

The background of this research is further grounded in the profound impact of geological disasters on communication infrastructure, particularly in regions like China. According to the 2023 Bulletin of China's Natural Resources, the country recorded 3,668 geological disasters in a single year [2]. These disasters, including earthquakes, landslides, and debris flows, often lead to the collapse of communication towers, power outages, and damage to fiber-optic cables, severely impeding disaster response efforts. In remote and mountainous areas, where terrestrial communication infrastructure is sparse, satellite communication systems play a pivotal role in maintaining connectivity. However, these systems are also vulnerable to disruptions caused by adverse weather conditions and physical barriers, highlighting the need for more resilient solutions.

The existing MMwave-MIMO technology in 5G faces obstacles in both design and performance. Managing precoding and beamforming methods becomes significantly more complex when large numbers of antennas are involved. In addition, while mmWave signals offer considerable advantages, they are highly susceptible to path loss, particularly when encountering physical barriers. This susceptibility frequently leads to signal degradation or loss, especially in areas where transmission must navigate through complex environments [3]. The above problems will cause difficulty in the disaster response and recovery scenario.

Reconfigurable Intelligent Surfaces (RIS) technology presents a transformative solution to these challenges. Unlike conventional relay systems, RIS provides a cost-effective and energy-efficient approach by dynamically manipulating electromagnetic properties such as phase and amplitude to optimize signal propagation. This capability not only improves signal quality but also extends coverage, mitigates interference, and improves the overall reliability of the system [4] [5]. The integration of RIS into Low Earth Orbit (LEO) satellite networks, which are increasingly deployed for high-speed internet and low-latency communication, offers a unique opportunity to address the energy and spectral efficiency challenges inherent in these networks. By leveraging RIS, we can reduce power consumption and spectral congestion associated with the growing number of satellites in LEO constellations, thereby enhancing the performance of satellite communication systems in disaster relief scenarios [6].

III. Project Introduction

The primary aim of this project is to enhance signal quality in B5G wireless communication systems by leveraging the capabilities of Reconfigurable Intelligent Surfaces (RIS). The project involves the design and simulation of a RIS-assisted multiple-input single-output (MISO) downlink system, where the base station transmits signals to a single user with the assistance of RIS. The system model considers both direct and RIS-reflected signal paths, with the goal of maximizing the network sum rate (NSR) as a performance metric.

The project's objectives include evaluating the properties of RIS, MIMO downlink systems, and beamforming techniques; designing a RIS-assisted MIMO downlink system model; proposing and testing optimization algorithms; and analyzing the performance of the system through simulation. The expected outcomes include the successful design and simulation of the RIS-assisted MIMO downlink system, the effectiveness of the proposed optimization algorithms, and the demonstration of RIS's ability to enhance signal quality in B5G wireless communication systems.

By addressing the challenges of signal quality, transmission distance, and energy efficiency, this project aims to contribute to the development of more robust and efficient B5G wireless networks, paving the way for future advancements in wireless communication technologies. Additionally, the integration of RIS into disaster response scenarios offers a promising solution to ensure uninterrupted connectivity during emergencies, thereby enhancing the overall resilience of communication systems in the face of natural disasters.

IV. Related Work

With the growing interest in reconfigurable intelligent surface (RIS) technology in low Earth orbit (LEO) satellite networks, its transformative potential in addressing the challenges of satellite-to-ground communication systems has become increasingly evident. Existing studies primarily focus on optimizing spectral efficiency, energy consumption, and coverage in LEO networks. However, traditional methods remain limited in scenarios such as urban canyons, high-mobility environments, and post-disaster communications. This section reviews prior research, identifies its limitations, and establishes the necessity of RIS-LEO integration, leading to our research contributions.

A. Key Challenges in LEO Satellite Communications

Despite their advantages of low latency and global coverage, LEO satellites face three major challenges:

1) **Line-of-Sight (LOS) Blockage:** Urban skyscrapers and geological obstacles (e.g., landslides, collapsed buildings) can disrupt direct satellite-to-ground links, rendering services unavailable.
2) **High Energy Consumption:** Frequent inter-satellite relaying and high-power beamforming significantly increase energy consumption, shortening the operational lifespan of satellites.
3) **Dynamic Network Topology:** The high mobility of LEO satellites, combined with unpredictable user distributions in disaster scenarios, complicates interference management and resource allocation.

Traditional techniques such as massive multiple-input multiple-output (MIMO) and non-orthogonal multiple access (NOMA) provide only partial solutions. For instance, [7] proposed a full-frequency reuse (FFR) scheme based on statistical channel state information (CSI) to enhance data rates. However, this approach struggles with LOS blockage in urban canyon environments. Similarly, [8] integrated RIS with NOMA to reduce power consumption by 54.9%, but it neglected the coupling effects between RIS phase adjustments and multi-user spatial interference, limiting overall system optimization. These shortcomings highlight the need for an innovative RIS-assisted architecture to address the complexities of LEO satellite communications.

B. Current Applications of RIS in Satellite Networks

RIS, with its ability to passively manipulate electromagnetic waves, offers unprecedented flexibility in overcoming LOS constraints. While early studies have demonstrated the potential of RIS in terrestrial wireless networks, its application in LEO satellite networks remains in its nascent stages.

[9] proposed a multi-user RIS-assisted framework that jointly optimizes beamforming and RIS phase shifts to improve urban coverage, achieving a 40% throughput gain. However, this study assumes static user distributions, making it unsuitable for highly mobile or disaster-stricken environments. Additionally, the adopted alternating optimization (AO) algorithm has a slow convergence rate, limiting real-time adaptability.

Meanwhile, [10] introduced a deep reinforcement learning (DRL)-based energy-efficient routing scheme that reduces LEO network energy consumption while meeting latency constraints. However, this method relies on medium Earth orbit (MEO) satellites for centralized control, introducing additional latency and single-point failure risks. Furthermore, it does not account for physical-layer challenges such as signal attenuation.

Overall, existing studies exhibit a disconnect between physical-layer (e.g., beamforming) and network-layer (e.g., routing) optimization, failing to achieve cross-layer coordination and adaptability to complex disaster scenarios.

C. Necessity of RIS-LEO Integration

Integrating RIS with LEO satellites offers three key advantages:

1) **Dynamic LOS Restoration:** By reflecting signals, RIS can create virtual LOS paths around obstacles, making it particularly effective in post-disaster areas where ground infrastructure is damaged.
2) **Energy Efficiency Optimization:** Unlike high-power active relays, RIS passively enhances signals through phase alignment, reducing satellite transmission power.
3) **Multi-User Interference Suppression:** The spatially selective reflection capability of RIS mitigates inter-user interference in dense networks, enhancing the cooperative gain of NOMA and beamforming techniques.

Despite its potential, existing RIS-assisted LEO research ([7], [9]) still suffers from two major limitations:

1) **Lack of Cross-Layer Optimization:** Current solutions fail to jointly optimize RIS phase shifts, user-satellite association, and beamforming, making it difficult to balance spectral efficiency, energy consumption, and coverage.
2) **Absence of Disaster Scenario Validation:** Most studies evaluate performance in stable urban environments, overlooking scenarios with infrastructure collapse and highly dynamic user mobility.

D. Our Contribution: Addressing the Gaps

To overcome these challenges, we propose a cross-layer optimized RIS-LEO framework tailored for disaster scenarios. By jointly considering beamforming, user-LEO association, and RIS phase adjustments, our approach achieves the following breakthroughs:

1) **Hybrid AO-SDR Algorithm:** By integrating semidefinite relaxation (SDR) with the AO algorithm, we aim to improve the solving speed of non-convex problems, enhancing adaptability to satellite mobility and channel variations.
2) **Disaster-Aware User Association Mechanism:** Our approach dynamically prioritizes emergency users (e.g., rescue teams) to ensure critical communication needs—an aspect neglected in existing research.
3) **Energy-Latency Trade-Off Optimization:** Unlike [10], which focuses solely on network-layer energy efficiency, our framework also aim to reduce satellite transmission power to meeting end-to-end latency constraints.

V. Model Design

A. System parameter

In the system , there are multi-antenna ultradense LEO satellites Base Station L denoted by $L \in \{1, 2, 3, ..., L\}$, with each satelite has the N antenna $N \in \{1, 2, 3, ..., N\}$. Single antenna BS serves users in T clusters $T \in \{1, 2, 3, ..., T\}$. For simplification, we assume there is only one user in each cluster.

There are M Reconfigurable Intelligent Surfaces (RIS) deployed in the system with uniform planar array (UPA) with horizantal number and vertical number $M = M_x \times M_y$. The RIS phase shift matrix [11] is a diagonal matrix given by M × M, which expressed as:

$$\mathbf{\Theta} = \mathrm{diag}\left(\theta_1, \cdots, \theta_\mathrm{n}\right), n \in [1, N] \tag{1}$$

The phase shift coefficients of element in this diagonal matrix can be expressed as amplitude and phase shift respectively.

$$\theta_n = \beta_n e^{j\varphi_n}, \quad \varphi_n \in [0, 2\pi], \quad \beta_n \in [0, 1] \tag{2}$$

In this paper, we assume $|\beta n| = 1$ without loss of generality. In this case, the communcation channel can be expressed by complex matrix. $H \in C^{N \times M}$ represent the channel matrix from the RIS to the LEO satellite. The vector $h_{R,T} \in C^{M \times 1}$ denotes the channel from the cluster to the RIS, which includes users i and j. Meanwhile, $h_{D,T} \in C^{N \times 1}$ describes the direct channel from the cluster to the satellite.

In signal transmission, the input signal is determined by direction and magnitude, and the direction is optimized by subsequent beamforming methods. the input signal can be expessed as

$$s_n = \sum_{N=1}^{T} w_n x_n k \tag{3}$$

where w_n represents the signal intended for user beamforming weight vector, x_n represents the input signal strength, k from LEO satellite is a binary association indicator, where k = 1 indicates that user is connected to LEO satellite, k = 0 otherwise.

Additive White Gaussian Noise (AWGN) was added to the channel, which expressed as

$$n \sim CN(0, \sigma^2) \tag{4}$$

B. Channel state information analysis

We focus on channel fading to maintain signal quality. However, in RIS-aided systems, estimating channels separately for RIS-LEO and cluster-RIS links is challenging due to scaling ambiguity. RIS passively reflects signals, intertwining the effects of its settings with the actual propagation. By modeling the overall link as a cascade channel, we combine the effects of both segments and bypass the ambiguity, the channel is simplified as [9]

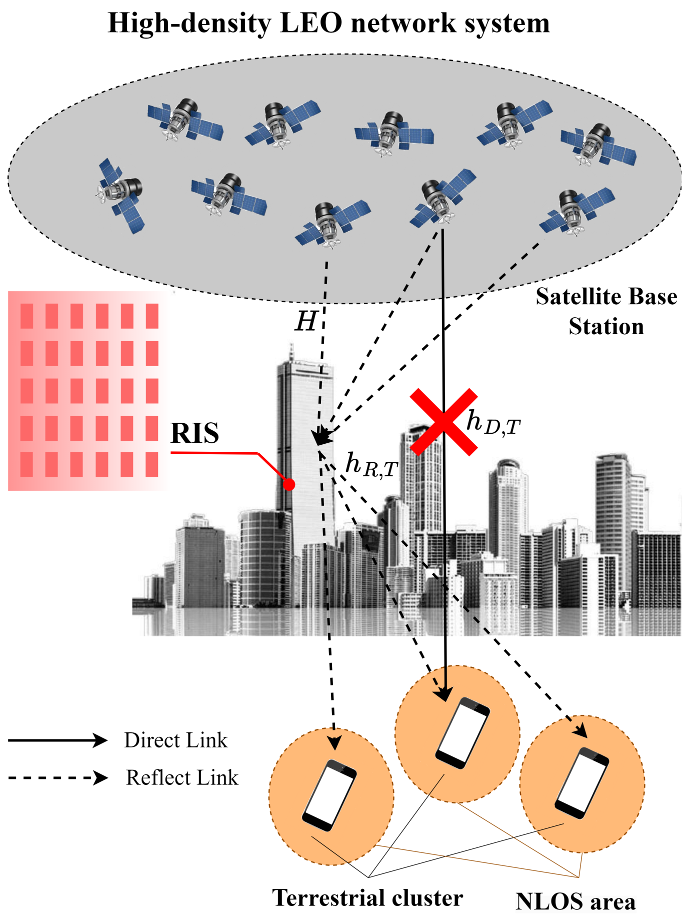

Fig. 1: LEO-RIS downlink model

$$y_T = (\mathbf{h}_{\mathrm{R},T}\Theta\mathbf{H} + h_{\mathrm{D},T})s + n_k \tag{5}$$

C. Fading model

In LEO system, fading gain can be elaborated as [12]

$$h = \sqrt{G_L G_R}\frac{c}{4\pi f_c d} \tag{6}$$

where c is speed of light, f is the frequency of wave. G_L denotes the transmit gain, G_R denotes the received gain.

Transmit antenna gain primarily relies on the radiation pattern and the geographical location, which can be approximately as [12]

$$\begin{aligned} G_L &= G_{max}\left(\frac{J_1(\theta)}{2\theta} + 36\frac{J_3(\theta)}{\theta^3}\right) \\ \theta &= 2.071\frac{\sin(\theta)}{\sin(\theta_{3dB})} \end{aligned} \tag{7}$$

This fomular adopts the first-kind Bessel functions with orders 1 and 2, respectively, where $G_m ax$ represents the maximum gain observed at the beam center. θ shows the center of the LEO satellite beam for a given location of users with the angle of 3dB loss relative to the beam's center is given by.

Due to shading in NLOS, G_R uses the Rayleigh fading model and can be expressed as [11]

$$G_R = \sqrt{L}\left(\sqrt{\frac{K_1}{K_1+1}}\mathbf{h}_G^{\mathrm{NLOS}} + \sqrt{\frac{1}{K_1+1}}\mathbf{h}_G^{\mathrm{NLOS}}\right) \tag{8}$$

VI. Transmit Power Optimization

To optimize for minimizing the total transmit power of satellite while enhancing downlink sum rate through joint optimization of beamforming, user-satellite associations, and RIS phase shifts, we need to adjust the formulation to include constraints on minimizing total transmit power.

Objective function: Minimize the total transmit power

$$\text{Minimum} \sum_{i=1}^{L}\sum_{j=1}^{T} x_{i,j}\left\|w_{ij}\right\|^2 \tag{9}$$

Constraints:

Power Constraints: Limit the total transmit power for each satellite

$$0 \leq \sum_{j=1}^{T} x_{i,j}\left\|w_{ij}\right\|^2 \leq P_0, \quad \forall i \in \{1,\ldots,L\} \tag{10}$$

Rate Constraints: Ensure each user's transmission rate meets a predefined threshold R_0

$$R_{ij} \geq R_0, \quad \forall i \in \{1,\ldots,L\}, \forall j \in \{1,\ldots,T\} \tag{11}$$

Association Constraints: Each cluster is associated with exactly one satellite

$$\begin{gathered}\sum_{i=1}^{L} x_{ij} = 1, \quad \forall j \in \{1,\ldots,T\} \\ x_{ij} \in \{0,1\}, \quad \forall i \in \{1,\ldots,L\}, \forall j \in \{1,\ldots,T\}\end{gathered} \tag{12}$$

RIS Phase Shift Matrix Constraints:

$$\begin{gathered}\Theta_{i,j} = 0, \quad \forall i \neq j, \quad \forall i,j \in \{1,\ldots,M\} \\ |\Theta_{i,i}| = 1, \quad \forall i \in \{1,\ldots,M\}\end{gathered} \tag{13}$$

Thus, the total power optimization for satellite can expressed as

$$\begin{aligned}
&\min_{w_L,T,x_{ij},\Theta} \quad \sum_{i=1}^{L}\sum_{j=1}^{T} x_{ij}\|w_{ij}\|^2 \\
&\text{s.t.} \\
&0 \leq \sum_{j=1}^{T} x_{ij}\|w_{ij}\|^2 \leq P_0, \quad \forall i \in \{1,\ldots,L\} \\
&R_{ij} \geq R_0, \quad \forall i \in \{1,\ldots,L\}, \forall j \in \{1,\ldots,T\} \\
&\sum_{i=1}^{L} x_{ij} = 1, \quad \forall j \in \{1,\ldots,T\} \\
&x_{ij} \in \{0,1\}, \quad \forall i \in \{1,\ldots,L\}, \forall j \in \{1,\ldots,T\} \\
&\Theta_{i,j} = 0, \quad \forall i \neq j, \quad \forall i,j \in \{1,\ldots,M\} \\
&|\Theta_{i,i}| = 1, \quad \forall i \in \{1,\ldots,M\}
\end{aligned} \tag{14}$$

A. *Optimization by AO Approach*

The transmit power optimization can be divided into three subproblems. The AO algorithm optimizes the transmit beamforming at LEO satellites, user association, and RIS phase shifts, refining each parameter in an alternating manner until convergence is reached, which ensures comprehensive optimization.

Beamforming optimization

This subproblem encapsulates the task of enhancing directional transmission to maximize system efficiency. When user association variables x and RIS phase shift are held fixed, the original problem transforms into a subproblem focused on optimizing beamforming. Here, w denotes the variable undergoing optimization to refine the beamforming strategy

$$\begin{aligned} &\min_{w_{i,j}} \quad \sum_{i=1}^{L}\sum_{j=1}^{T} x_{i,j}\|w_{i,j}\|^2 \\ &\text{s.t.} \quad 0 \leq \sum_{j=1}^{T} x_{i,j}\|w_{i,j}\|^2 \leq P_0, \quad \forall i \in \mathcal{L} \\ &\sum_{i=1}^{L} R_{i,j} \geq r_0, \quad \forall j \in \mathcal{T} \end{aligned} \tag{15}$$

Association optimization

This optimization underscores the importance of establishing a one-to-one constrained correspondence between satellites and clusters. When user beam-forming variables w and RIS phase shift are held, the original problem transforms into a subproblem focused on association variables x

$$\begin{aligned} &\min_{x_{i,j}} \quad \sum_{i=1}^{L}\sum_{j=1}^{T} x_{i,j}\|w_{i,j}\|^2 \\ &\text{s.t.} \quad \sum_{j=1}^{K} x_{i,j}\|w_{i,j}\|^2 \leq P_0, \quad \forall i \in \mathcal{L} \\ &\sum_{i=1}^{L} x_{i,j} = 1, \quad \forall j \in \mathcal{T} \\ &x_{i,j} \in \{0,1\}, \quad \forall i \in \mathcal{L}, j \in \mathcal{T} \end{aligned} \tag{16}$$

This subproblem represents an integer programming problem with a non-convex objective function. However,it can be transformed into a many-to-one matching problem. a greedy approach is employed to optimize the matching scheme, where each terrestrial user is paired with the most preferred LEO satellite, and each association is added to the set.

RIS shift optimization

When user beam-forming variables w and association variables x are held, the original problem transforms into a subproblem focused on RIS phase θ

$$\begin{aligned} &\min_{\theta} \quad \sum_{i=1}^{L}\sum_{j=1}^{T} x_{i,j}\|w_{ij}\|^2 \\ &\text{s.t.} \quad \sum_{i=1}^{L} R_{i,j} \geq r_0, \quad \forall j \in \mathcal{T}, \\ &\Theta_{i,j} = 0, \quad \forall i \neq j, \quad \forall i,j \in \{1,\ldots,M\} \\ &|\Theta_{i,i}| = 1, \quad \forall i \in \{1,\ldots,M\} \end{aligned} \tag{17}$$

With the particularity of RIS shift, the cascaded channel can be directly converted into the reflected channel because of the reduction of channel ambiguity. Therefore, the channel is divided into direct channel $\mathbf{b}_{i,j}$ and reflection channel $\mathbf{a}_{i,j}$.

$$\begin{aligned} \mathbf{a}_{i,j} &= \sum_{i=1}^{L} \operatorname{diag}(\mathbf{I}_{R_{i,j}})\mathbf{H}_i x_{i,R} \cdot \sum_{i'=1}^{L} \mathbf{w}_{i',j} x_{i',j} \\ \mathbf{b}_{i,j} &= \sum_{i=1}^{L} g_{i,j} x_{i,j} \cdot \sum_{i'=1}^{L} \mathbf{w}_{i',j} x_{i',j} \end{aligned} \tag{18}$$

AO optimization interation

Now we decompose the overarching problem into manageable subproblem. The AO algorithm systematically dissects the initial problem into distinct subproblems and addressing specific optimization variables. With iteration, commencing from the initialization phase, this method progressively refine these variables in the i-th iteration. Leveraging solutions from the preceding iteration, we iteratively calculate the updated variables by solving the respective subproblems. This iterative journey persists until specific convergence criteria are met, a hallmark of the AO algorithm, which exhibits provable convergence under certain conditions. Through this iterative approach, the complexities of the overarching problem are effectively managed. With each iteration, commencing from the initialization phase where variables $x^{(0)}, w^{(0)}$, and $\Theta^{(0)}$ are set, we progressively refine these variables in the i-th iteration. Leveraging solutions from the preceding iteration ($x^{(i-1)}, w^{(i-1)}$, and $\Theta^{(i-1)}$), we iteratively calculate$x^{(i)}, w^{(i)}$, and $\Theta^{(i)}$ by solving the respective subproblems.

B. Optimization by SDR Approach

Semidefinite relaxation (SDR) can be implemented for optimizing phase shifts under constraint, particularly for continuous phase shifts defined as VV^H. V comprises the diagonal elements of the RIS phase matrix θ. Then, the unit modulus constraint can be equivalently expressed as $V \succ 0$ and rank(V)=1. However, due to the rank one constraint, the transformed problem remains non-convex. The SDR method addresses this by removing the non-convex rank one constraint. This result becomes a convex semidefinite program (SDP). Then it can be solved by CVX toolbox.

Since SINR increases with signal strength γ, the SDR optimize γ directly for signal quality. Combining with the methods mentioned in AO, we optimize w and x in advance by AO method. This simplifies the problem to:

$$\begin{aligned}
&w^* = \sqrt{p}\frac{\|h_{R,T}^H \Theta G + h_{R,T}^H\|}{(h_{R,T}^H \Theta G + h_{R,T}^H)^H} \triangleq w_{MRT} \\
&V = [v_1, v_2, \dots, v_n]^H \\
&v_n = e^{j\theta_n}, \quad \forall n \\
&|v_n| = 1 \\
&h_{R,T}^H \Theta G = V^H \theta
\end{aligned} \tag{19}$$

After transformation and expansion, it can be observed that the problem is a non-convex second-order constrained quadratic programming problem.

$$\max_v V^H \theta \theta^H V + V^H \theta h_{D,T} + h_{D,T}^H V^H \theta \tag{20}$$

By introducing auxiliary variables and transformations, the problem is reformulated into a standard convex SDP problem. However, typically, the relaxed problem may not yield a rank-one solution, meaning rank not equal to 1, and it has an upper bound but no optimal solution [13].

$$\begin{aligned}
&\max_{\overline{V}} \overline{V}^H R \overline{V} = tr(R\overline{V}\overline{V}^H) \\
&s.t. \mathbf{V} = \begin{bmatrix} \mathbf{v}\mathbf{v}^H & \mathbf{v}^H \\ \mathbf{v} & 1 \end{bmatrix} \\
&\sigma = \overline{V}\overline{V}^H \\
&\max_{\sigma} R\sigma \\
&s.t. \sigma \succ= 0
\end{aligned} \tag{21}$$

Therefore, additional steps are required to construct a rank-one solution from the optimal solution of problem with higher rank. Specifically, do eigenvalue decomposition to V, resulting in a matrix of size (N+1)×(N+1). Consequently, we can obtain a sub-optimal solution to achieve the purpose of eliminating one phase shift variable.

VII. Sum Rate Optimization

This optimization problem is subject to constraints including the rate, satellite transmit power limits, and permissible user-to-satellite associations. The objective is to maximize the total downlink sum rate under these conditions.
Objective Function: Maximize the downlink sum rate:

$$\text{Maximize} \quad \sum_{i=1}^{L} \sum_{j=1}^{T} x_{i,j} \log_2 \left(1 + \frac{|y_{T,i}^H \mathbf{w}_{c,T,i}|^2}{\sum_{k \neq T}^{T} |y_T^H \mathbf{w}_{c,T}|^2 + |y_{T,j}^H \mathbf{w}_{r,T,j}|^2 + \sigma^2} \right) \tag{22}$$

Constraints:
Power Constraints: Limit the total transmit power for each satellite

$$0 \le \sum_{j=1}^{T} x_{i,j} \|w_{ij}\|^2 \le P_0, \quad \forall i \in \{1, \dots, L\} \tag{23}$$

Rate Constraints: Ensure each user's transmission rate meets a predefined threshold R_0

$$R_{ij} \ge R_0, \quad \forall i \in \{1, \dots, L\}, \forall j \in \{1, \dots, T\} \tag{24}$$

Association Constraints: Each cluster is associated with exactly one satellite

$$\begin{aligned}\sum_{i=1}^{L} x_{ij} = 1, \quad \forall j \in \{1,\ldots,T\} \\ x_{ij} \in \{0,1\}, \quad \forall i \in \{1,\ldots,L\}, \forall j \in \{1,\ldots,T\}\end{aligned} \tag{25}$$

RIS Phase Shift Matrix Constraints:

$$\begin{aligned}\Theta_{i,j} = 0, \quad \forall i \neq j, \quad \forall i,j \in \{1,\ldots,M\} \\ |\Theta_{i,i}| = 1, \quad \forall i \in \{1,\ldots,M\}\end{aligned} \tag{26}$$

Thus, the sum rate optimization for satellite can expressed as

$$\begin{aligned}&\max_{\mathbf{w}_{c,T}, x_{i,j}, \Theta} \sum_{i=1}^{L}\sum_{j=1}^{T} x_{i,j} \log_2\left(1 + \frac{\left|y_{T,i}^{H}\mathbf{w}_{c,T,i}\right|^2}{\sum_{j\neq T}^{T}\left|y_{T,j}^{H}\mathbf{w}_{c,T}\right|^2 + \left|y_{T,j}^{H}\mathbf{w}_{r,T,j}\right|^2 + \sigma^2}\right) \\ &\text{s.t.} \\ &0 \leq \sum_{j=1}^{T} x_{ij}\|w_{ij}\|^2 \leq P_0, \quad \forall i \in \{1,\ldots,L\} \\ &R_{ij} \geq R_0, \quad \forall i \in \{1,\ldots,L\}, \forall j \in \{1,\ldots,T\} \\ &\sum_{i=1}^{L} x_{ij} = 1, \quad \forall j \in \{1,\ldots,T\} \\ &x_{ij} \in \{0,1\}, \quad \forall i \in \{1,\ldots,L\}, \forall j \in \{1,\ldots,T\} \\ &\Theta_{i,j} = 0, \quad \forall i \neq j, \quad \forall i,j \in \{1,\ldots,M\} \\ &|\Theta_{i,i}| = 1, \quad \forall i \in \{1,\ldots,M\}\end{aligned} \tag{27}$$

A. *Optimization by AO Approach*

Similarly to transmit power optimization, the sum rate optimization can also be divided into three subproblems.

Beamforming optimization This subproblem encapsulates the task of enhancing directional transmission to maximize system efficiency. When user association variables x and RIS phase shift are held fixed, the original problem transforms into a sub-problem focused on optimizing beamforming. Here, w denotes the variable undergoing optimization to refine the beamforming strategy

$$\begin{aligned}&\max_{w_{i,j}} \sum_{i=1}^{L}\sum_{j=1}^{T} Ri,j \\ &\text{s.t.} \sum_{j=1}^{T} x_{i,j}\|w_{i,j}\|^2 \leq P_0, \quad \forall i \in \mathcal{L} \\ &\sum_{i=1}^{L} R_{i,j} \geq r_0, \quad \forall j \in \mathcal{T}\end{aligned} \tag{28}$$

Here, an auxiliary variable t is introduced, where tt^H represents the optimization beamforming variable. This auxiliary variable aids in formulating the optimization problem, refining the beamforming strategy [14].

$$
\begin{aligned}
&\max_{w_{i,j},t_{i,j}} \sum_{i=1}^{L}\sum_{j=1}^{T}\log_2 t_{i,j}\\
&\text{s.t.} \sum_{i=1}^{L} t_{i,j} \geq 2^{r_0} \quad \forall j \in T\\
&\sum_{j=1}^{T} x_{i,j}\|w_{i,j}\|^2 \leq P_0, \quad \forall i \in \mathcal{L}\\
&t_{i,j} \leq \frac{\left|\mathbf{h}_{i,j}\mathbf{w}_{i,j}\right|^2}{\sum\limits_{i'=1}^{L}\sum\limits_{i'\neq k} x_{i',j'}\left|\mathbf{h}_{i,j}\mathbf{w}_{i',j'}\right|^2+\sigma^2}+1 \quad \forall i \in \mathcal{L}, k=j \in T
\end{aligned} \tag{29}
$$

Association optimization

This optimization underscores the importance of establishing a one-to-one constrained correspondence between satellites and clusters. When user beam-forming variables w and RIS phase shift are held, the original problem transforms into a subproblem focused on association variables x

$$
\begin{aligned}
&\max_{x_{i,j}} \sum_{i=1}^{L}\sum_{j=1}^{T} Ri,j\\
&\text{s.t.} \quad \sum_{j=1}^{K} x_{i,j}\|w_{i,j}\|^2 \leq P_0, \quad \forall i \in \mathcal{L}\\
&\sum_{i=1}^{L} x_{i,j} = 1, \quad \forall j \in \mathcal{T}\\
&x_{i,j} \in \{0,1\}, \quad \forall i \in \mathcal{L}, j \in \mathcal{T}
\end{aligned} \tag{30}
$$

This subproblem represents an integer programming problem with a non-convex objective function. However,it can be transformed into a many-to-one matching problem. a greedy approach is employed to optimize the matching scheme, where each terrestrial user is paired with the most preferred LEO satellite, and each association is added to the set.

RIS shift optimization

When user beam-forming variables w and association variables x are held, the original problem transforms into a subproblem focused on RIS phase θ

$$
\begin{aligned}
&\max_{\theta} \sum_{i=1}^{L}\sum_{j=1}^{T} Ri,j\\
&\text{s.t.} \quad \sum_{i=1}^{L} R_{i,j} \geq r_0, \quad \forall j \in \mathcal{T},\\
&\Theta_{i,j} = 0, \quad \forall i \neq j, \quad \forall i,j \in \{1,\ldots,M\}\\
&|\Theta_{i,i}| = 1, \quad \forall i \in \{1,\ldots,M\}
\end{aligned} \tag{31}
$$

With the particularity of RIS shift, the cascaded channel can be directly converted into the reflected channel because of the reduction of channel ambiguity. Therefore, the channel is divided into direct channel $\mathbf{b}_{i,j}$ and reflection channel $\mathbf{a}_{i,j}$.

$$
\begin{aligned}
\mathbf{a}_{i,j} &= \sum_{i=1}^{L} \operatorname{diag}(\mathbf{I}_{R_{i,j}})\mathbf{H}_i x_{i,R} \cdot \sum_{i'=1}^{L} \mathbf{w}_{i',j} x_{i',j}\\
\mathbf{b}_{i,j} &= \sum_{i=1}^{L} g_{i,j} x_{i,j} \cdot \sum_{i'=1}^{L} \mathbf{w}_{i',j} x_{i',j}
\end{aligned} \tag{32}
$$

AO optimization interation

Similar to transmit power optimization, now we decompose the overarching problem into manageable subproblem. The AO algorithm systematically dissects the initial problem into distinct subproblems and addressing specific optimization variables. With iteration, commencing from the initialization phase, this method progressively refine these variables in the i-th iteration. Leveraging solutions from the preceding iteration, we iteratively calculate the updated variables by solving the respective subproblems. This iterative journey persists until specific convergence criteria are met, a hallmark of the AO algorithm, which exhibits provable convergence under certain conditions. Through this iterative approach, the complexities of the overarching problem are effectively managed. With each iteration, commencing from the initialization phase where variables $x^{(0)}, w^{(0)}$, and $\Theta^{(0)}$ are set, we progressively refine these variables in the i-th iteration. Leveraging solutions from the preceding iteration ($x^{(i-1)}, w^{(i-1)}$, and $\Theta^{(i-1)}$), we iteratively calculate $x^{(i)}, w^{(i)}$, and $\Theta^{(i)}$ by solving the respective subproblems.

B. Optimization by SDR Approach

For the phase-based non-convex optimization, it is divided into two parts. First, by introducing variables by SDR to reduce the constraint, the problem is simplified for Gaussian solving. Second, for the size distribution of the RIS array, the On-off Scheme is employed. This scheme, as adopted, toggles reflecting elements on and off to minimize training overhead. Initially, all elements are off, allowing the base station to estimate the direct channel. Subsequently, in each following time slot, few element or group is switched on, while the others remain off, expressed as matrix. The formula is show corresponding optimization by introducing t, R, and V.

$$
\begin{aligned}
&R_k = B\log\left(1+\frac{\left|\mathbf{b}_{k,k}+\mathbf{v}^H\mathbf{a}_{k,k}\right|^2}{\sum_{j\neq k}\left|\mathbf{b}_{k,j}+\mathbf{v}^H\mathbf{a}_{k,j}\right|^2+\sigma^2}\right)\\
&t_k = 1+\frac{\left|\mathbf{b}_{k,k}+\mathbf{v}^H\mathbf{a}_{k,k}\right|^2}{\sum_{j\neq k}\left|\mathbf{b}_{k,j}+\mathbf{v}^H\mathbf{a}_{k,j}\right|^2+\sigma^2},\\
&\mathbf{R}_{k,j} = \begin{bmatrix}\mathbf{a}_{k,j}\mathbf{a}_{k,j}^H & \mathbf{a}_{k,j}\mathbf{b}_{k,j}^H\\ \mathbf{a}_{k,j}^H\mathbf{b}_{k,j} & 0\end{bmatrix},\\
&\mathbf{V} = \begin{bmatrix}\mathbf{v}\mathbf{v}^H & \mathbf{v}^H\\ \mathbf{v} & 1\end{bmatrix}.
\end{aligned} \tag{33}
$$

Here, V comprises the diagonal elements of the RIS phase matrix θ. The constraint on V requires it to be a semi-positive definite matrix with rank one. To handle the non-convex rank constraint, we relax it by introducing supplementary slack variables denoted as β_n. This transforms the original problem into a series of convex subproblems, which can be readily addressed.

$$
\begin{aligned}
&\max_{t_j,\mathbf{v}} \quad \sum_{j=1}^{T}\log_2 t_j,\\
&\text{s.t.} \quad \operatorname{tr}(\mathbf{R}_{j,j}\mathbf{V})+|\mathbf{b}_{j,j}|^2 \geq \frac{\psi_j}{2}\beta_j^2+\frac{1}{2\psi_j}(t_j-1)^2, \quad \forall j\in\mathcal{T},\\
&\sigma^2+\sum_{i\neq j}\left(\operatorname{tr}(\mathbf{R}_{i,j}\mathbf{V})+|\mathbf{b}_{i,j}|^2\right) \leq \beta_j, \quad \forall j\in\mathcal{T},\\
&\mathbf{V}_{n,n}=1, \quad \forall 1\leq n\leq M,\\
&\mathbf{V}\succeq 0,\\
&\psi_j = \frac{\left(t_j^{(i-1)}-1\right)}{\beta_j^{(i-1)}}, \quad \forall j\in\mathcal{T}.
\end{aligned} \tag{34}
$$

After solving for V, the RIS phase matrix Θ can be obtained through eigenvalue decomposition of V. Specifically, the diagonal elements of Θ can be generated by $v = UD^{-\frac{1}{2}}$, where D is the eigenvalue matrix of V and U is the combination of corresponding right eigenvectors.

VIII. MATLAB Works

A. AO method

In matlab simulation, AO iteration is performed through a multilayer loop to optimize w, x, $\Theta, for the fractional function,$ and the realized process design is shown in the following flow chart.

[1] AO$x_{\text{initial}}, w_{\text{initial}}, \Theta_{\text{initial}}, \epsilon$ Initialize variables: $x \leftarrow x_{\text{initial}}$, $w \leftarrow w_{\text{initial}}$, $\Theta \leftarrow \Theta_{\text{initial}}$, $i \leftarrow 1$ true $R_{\text{total\_old}} \leftarrow$ calculate_total_sum_rate(Θ $w \leftarrow$ solve_subproblem (Θ, x) $x \leftarrow$ calculate_x(Θ, w) $x \leftarrow$ update_xmn(x) $\Theta \leftarrow$ solve_subproblem_,(x, w) $R_{\text{total\_new}} \leftarrow$ calculate_total_sum_rate(Θ, w, x) $|R_{\text{total\_new}} - R_{\text{total\_old}}| < \epsilon$ **break** $i \leftarrow i+1$ **return** x, w, Θ

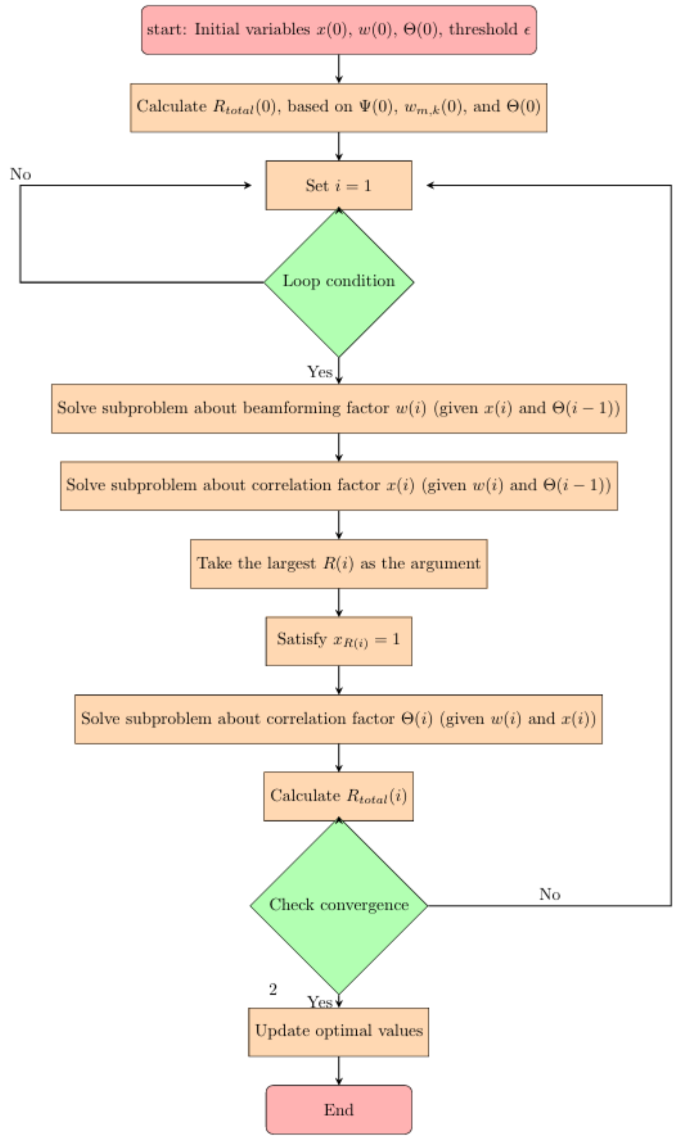

Fig. 2: AO method iteration

B. *CVX for SDR*

Perform SVD decomposition on matrix V, generate a random vector r, to approximate the upper bound, utilize CVX to optimize power and sum rate, maximizing the objective function, and ensuring constraints are satisfied. This process iterates to find the optimal solution.

[1] CVX coding

```
cvx begin
variable V(N+1,N+1) symmetric
maximize(trace(R*V))
subject to
for n=1:N+1
V(n,n)==1;
end
V == semidefinite(N+1);
cvx end
```

[2] SVD decomposition

```
[U,W,Z] = svds(V);
```

```
obj max = -80; // Initialize maximum objective value
n = length(W); // Number of singular values
// Loop to find maximum objective value
for j = 1: 500 // Generate a random complex vector r
r = sqrt(1/2) * (randn(n,1) + 1i * randn(n,1));
v = U * sqrt(W) * r; // Compute objective function value
obj = (v' * R * v); // Update maximum objective value
if obj ≤ objmax
objmax = obj;
v max = v;
end end
```

IX. Simulation Results

The software implementation predominantly utilized the MATLAB programming language. MATLAB was selected for its robust support in numerical computing, leveraging built-in capabilities for optimization (CVX) and multi-dimensional array operations in MATLAB. Iterative processes and multi-dimensional simulations were key functionalities adopted. The development platform was a Windows-based computer. The parameters for numerical Simulations are displayed as follows[6]:

Table 6.1: Parameter Values [6]

Parameter	**Value**
Rician factor for LOS channel	16 dB
Rayleigh factor for NLOS channel	0.22 dB
Frequency of carrier	18 GHz
Gaussian white noise	-174 dBm/Hz
Height of LEOs	600 km [6]
Number of LEOs	12000 [6]
Number of LEO satellite antennas	16
Gain of LEO satellite antennas	18 dBi

A. *Sum rate in power constraint*

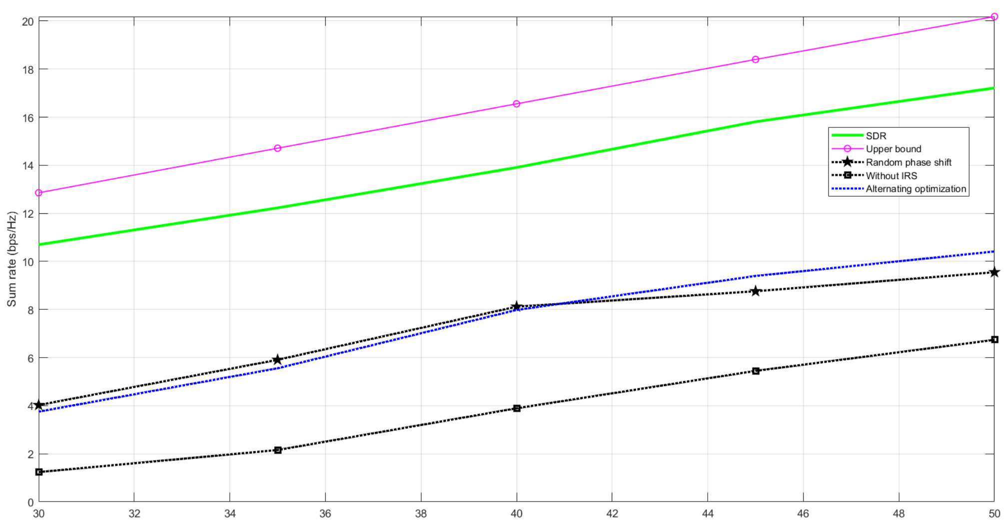

Fig. 3: Sum rate in power constraint for different methods

The performance of different methods in terms of sum rate are compared in Figure 3. First, the SDR method performed the best13bps/Hz increase than non-RIS system across all transmission power ranges, providing the highest sum rate, with a relatively stable growth trend as the transmission power increased. The theoretical upper bound curve lies above all methods, indicating that the SDR method is close to the theoretical optimal solution, but still has some gap (2.1 bps/Hz) and has not achieved complete optimization. Furthermore, the upper bound curve has a steeper slope, suggesting that there is more potential for sum rate improvement in the high power region. In contrast, the sum rates of the AO and random phase shift schemes are similar and clearly lower than that of the SDR optimization scheme, indicating that the convergence of the AO method is not fully achieved in this scenario. Nevertheless, these two schemes still perform better than the no-RIS system in both low and high power regions (2.3 bps/Hz). Finally, the no-RIS system has the lowest sum rate, further confirming the significant performance improvement brought by the introduction of RIS to the system

B. LEO power in rate constraint

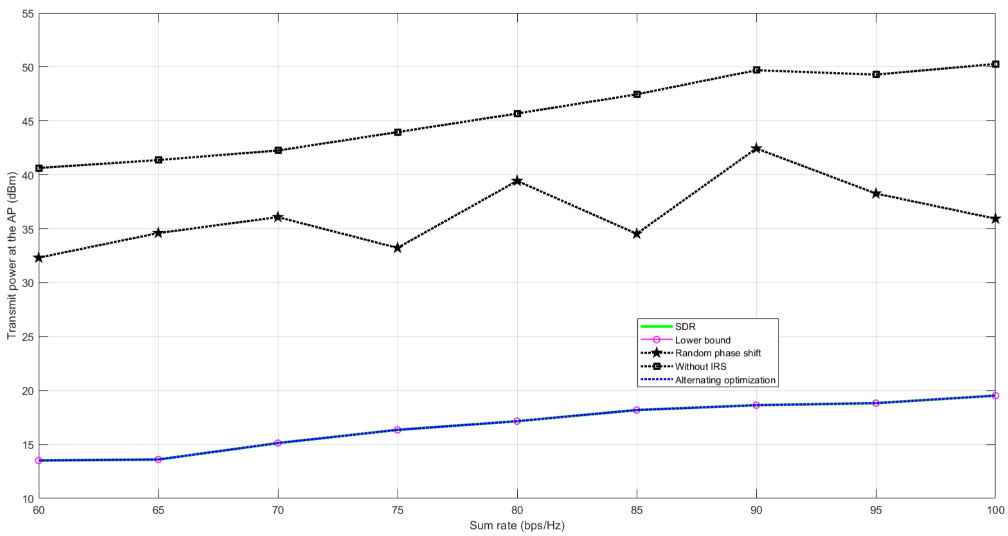

Fig. 4: Sum rate in power constraint for different methods

Figure 4 illustrates the minimum power needed for the LEO for sum rate demands. The RIS-assisted system optimized with SDR and AO significantly reduces power consumption, saving approximately 10-15 dBm compared to the non- RIS system at the same sum rate. Among the optimization methods, SDR and AO demonstrates the best performance, achieving the lowest power requirement across all sum rate ranges, Notably, the SDR and AO methods approaches the theoretical lowest bound, indicating that both solution are nearly optimal. Moreover, the required power grows nonlinearly with increasing sum rate demands. This growth is particularly steep in the high sum rate region (> 85 bps/Hz), emphasizing the high power cost associated with achieving extremely high data rates.

C. Power convergence for SDR and AO

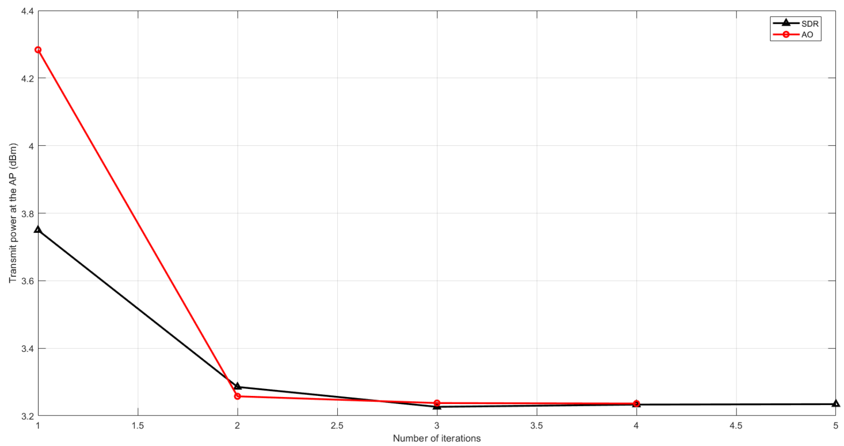

Fig. 5: Greart converges of AO/SDR for reducing total satelite power in LEO about 4/5 times

The experimental results show that both the SDR and AO algorithms significantly reduced the system's transmission power during the iterative process. The SDR algorithm stabilized after the 5th iteration, while the AO algorithm reached a stable state after the 4th iteration. Both algorithms reduced transmission power by 24% in fewer iterations, demonstrating efficient energy optimization. Although the SDR algorithm exhibited slightly faster initial convergence (in the second iteration) compared to the AO algorithm, both achieved nearly identical final transmission power, indicating similar performance in energy optimization. Overall, both SDR and AO algorithms are suitable for energy consumption optimization in LEO systems, as they can significantly reduce energy usage while maintaining system performance.

D. Mechine learning prediction

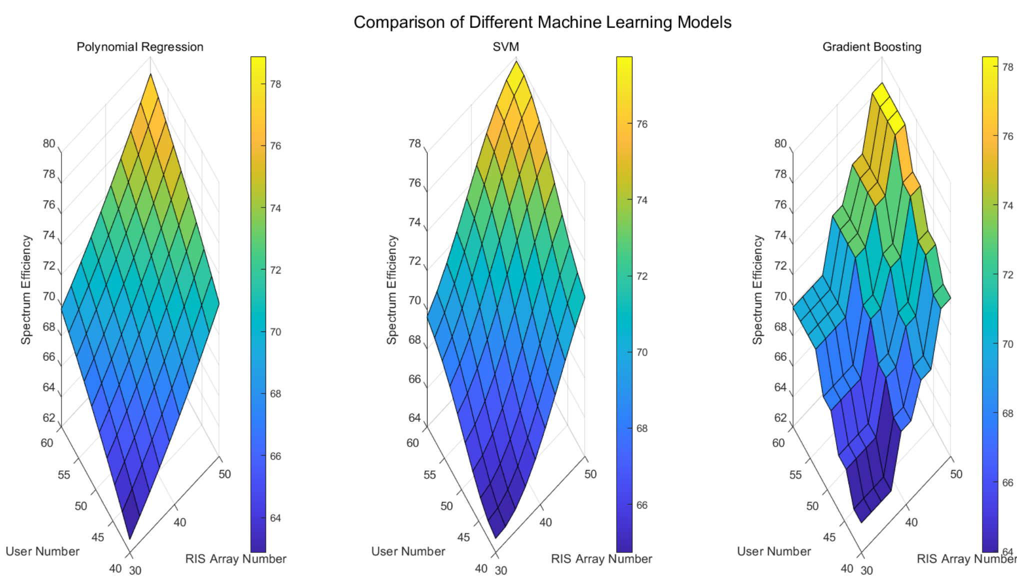

Fig. 6: Mechine Learning model for prediction

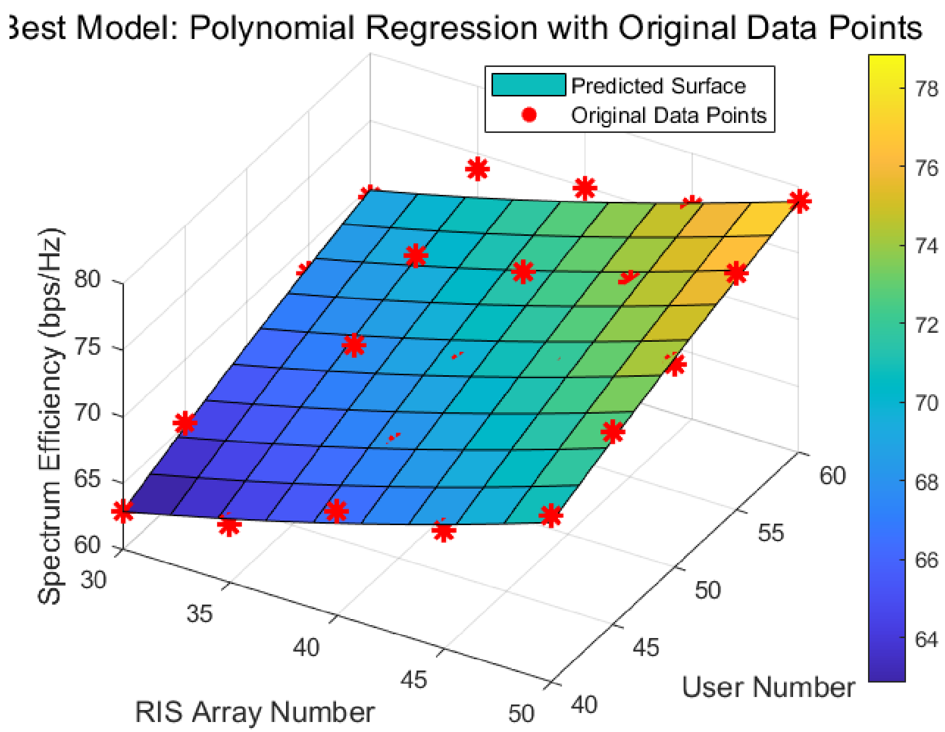

Fig. 7: Best model compared with original points

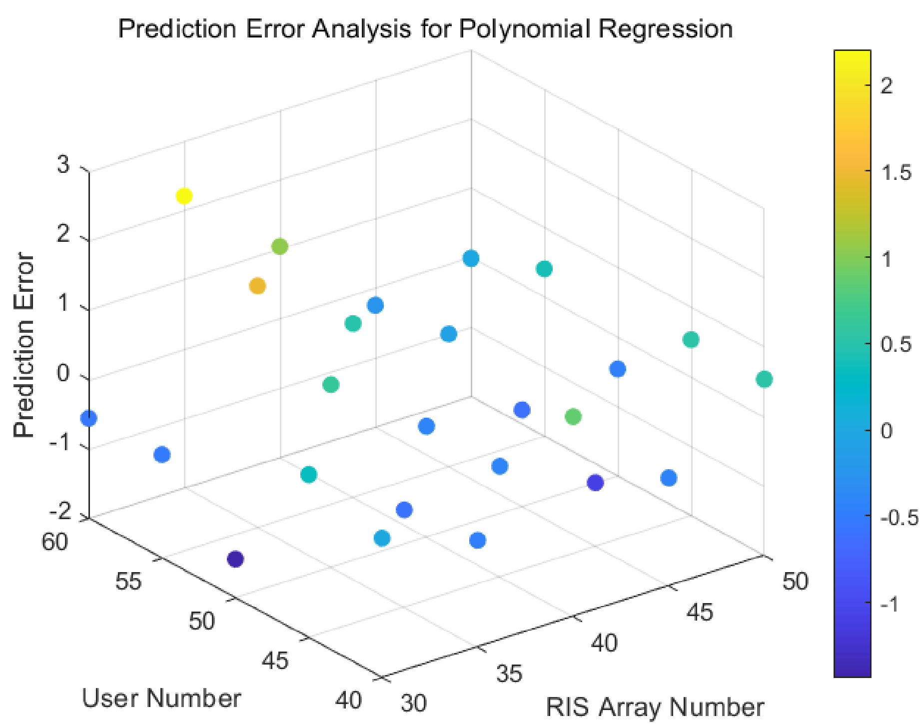

Fig. 8: Error analysis

The experimental results demonstrate that polynomial regression outperforms other machine learning approaches in predicting spectrum efficiency based on RIS array number and user number parameters. This model achieved the highest accuracy with a mean squared error (MSE) of 1.6368 and an R^2 score of 0.8917, compared to Support Vector Machine (SVM) (MSE: 2.1170,

R^2: 0.8600) and Gradient Boosting (MSE: 5.1323, R^2: 0.6605). The polynomial regression model successfully captures the nonlinear relationships between input parameters and spectrum efficiency, providing stable predictions across the entire input range as visualized in the 3D surface plots.

Further analysis reveals that both RIS array number and user number significantly impact spectrum efficiency, with higher values of both parameters generally corresponding to improved efficiency up to 78 bps/Hz. The prediction errors for the polynomial regression model remain consistently small, typically within ± 2 units across the parameter space. This model effectively reduces computational requirements compared to traditional AO iteration methods, decreasing processing time substantially while maintaining theoretical consistency. The smooth surface of the polynomial model, closely fitting the original data points, confirms its superior generalization capability and suitability for real-time spectrum efficiency prediction in RIS-enabled systems.

X. Conclusion

This research has successfully demonstrated the effectiveness of combining Reconfigurable Intelligent Surface (RIS) technology with machine learning approaches to optimize LEO satellite communication systems. The SDR-based optimization framework proved superior for sum rate optimization, delivering a substantial 13 bps/Hz increase compared to non-RIS systems across all transmission power ranges. Our analysis confirmed that RIS-assisted systems significantly reduce power consumption, with SDR and AO methods achieving 10-15 dBm power savings compared to conventional non-RIS configurations while approaching theoretical performance bounds. The convergence analysis revealed both SDR and AO algorithms efficiently reduce transmission power by 24% within 4-5 iterations, demonstrating excellent energy optimization capabilities. Additionally, our machine learning implementation, particularly the polynomial regression model with an R^2 score of 0.8917, successfully captured the nonlinear relationships between RIS array parameters and spectrum efficiency. This model enables real-time prediction capabilities while substantially reducing computational requirements compared to traditional iterative methods. These findings confirm that RIS technology, when coupled with appropriate optimization techniques, offers a promising solution for enhancing spectral efficiency, reducing power consumption, and improving overall performance in next-generation LEO satellite communication systems.

XI. Future WORK

Building upon our successful implementation of RIS-assisted LEO satellite communication systems, several promising research directions emerge that directly extend our findings:

- **Mobile RIS Implementation on UAVs:** Our conclusion highlighted the significant power savings ($10-15$ dBm) achieved with static RIS configurations. Extending this to UAV-mounted mobile RIS systems could potentially enhance these savings in dynamic environments while maintaining the rapid convergence ($4-5$ iterations) demonstrated in our research. This would be particularly valuable for emergency response scenarios in the geological disaster-prone areas identified in our market analysis.
- **Enhanced Machine Learning Integration:** While our polynomial regression model achieved an R^2 score of 0.8917, further improvements could be made by incorporating deep learning approaches to better capture the complex nonlinear relationships between system parameters. This would build upon our computational efficiency gains and further reduce prediction time compared to traditional iterative methods.
- **Joint Optimization Framework:** Our research demonstrated separate successes with SDR and AO methods. A unified optimization framework combining these approaches could potentially close the remaining gap (2.1 bps/Hz) between our achieved performance and the theoretical upper bound identified in our spectral efficiency analysis.
- **Multi-Satellite Coordination:** Expanding our single-satellite model to incorporate coordination among multiple LEO satellites would address the spectrum congestion concerns mentioned in our market analysis, leveraging our proven RIS optimization techniques to manage inter-satellite interference.

These research directions directly build upon the demonstrated 13 bps/Hz improvement over non-RIS systems and 24% power reduction achieved in our study, with the goal of further enhancing spectral efficiency and reducing power consumption in next-generation LEO satellite communication systems.

References

[1] S. Zhang, Q. Wu, S. Xu, and G. Y. Li, "Fundamental green tradeoffs: Progresses, challenges, and impacts on 5g networks," *IEEE Communications Surveys Tutorials*, vol. 19, no. 1, pp. 33–56, 2017.

[2] Q. Wu, G. Y. Li, W. Chen, D. W. K. Ng, and R. Schober, "An overview of sustainable green 5g networks," *IEEE Wireless Communications*, vol. 24, no. 4, pp. 72–80, 2017.

[3] T. Kebede, Y. Wondie, J. Steinbrunn, H. B. Kassa, and K. T. Kornegay, "Precoding and beamforming techniques in mmwave-massive mimo: Performance assessment," *IEEE Access*, vol. 10, pp. 16 365–16 387, 2022.

[4] X. Cao, Q. Chen, T. Tanaka, M. Kozai, and H. Minami, "A 1-bit time-modulated reflectarray for reconfigurable-intelligent-surface applications," *IEEE Transactions on Antennas and Propagation*, vol. 71, no. 3, pp. 2396–2408, 2023.

[5] L. Yang, J. Yang, W. Xie, M. O. Hasna, T. Tsiftsis, and M. D. Renzo, "Secrecy performance analysis of ris-aided wireless communication systems," *IEEE Transactions on Vehicular Technology*, vol. 69, no. 10, pp. 12 296–12 300, 2020.

[6] S. Hu, F. Rusek, and O. Edfors, "Beyond massive mimo: The potential of data transmission with large intelligent surfaces," *IEEE Transactions on Signal Processing*, vol. 66, no. 10, pp. 2746–2758, 2018.

[7] L. You, K.-X. Li, J. Wang, X. Gao, X.-G. Xia, and B. Ottersten, "Massive mimo transmission for leo satellite communications," *IEEE Journal on Selected Areas in Communications*, vol. 38, no. 8, pp. 1851–1865, 2020.

[8] J.-I. Lee, Y.-H. Hsu, and S.-S. Sun, "A drl-based noma power allocation scheme for leo satellite networks," in *2024 IEEE 100th Vehicular Technology Conference (VTC2024-Fall)*, 2024, pp. 1–5.

[9] X. Zhang, T. Ma, X. Qin, Y. Wang, and H. Zhou, "Reflecting intelligent surface aided downlink transmission in ultra-dense leo satellite networks," in *2023 IEEE 23rd International Conference on Communication Technology (ICCT)*, 2023, pp. 1123–1128.

[10] Y.-H. Hsu, J.-I. Lee, and F.-M. Xu, "A deep reinforcement learning based routing scheme for leo satellite networks in 6g," in *2023 IEEE Wireless Communications and Networking Conference (WCNC)*, 2023, pp. 1–6.

[11] M. Shen, X. Lei, P. Takis Mathiopoulos, X. Tang, R. Qingyang Hu, and P. Fan, "Robust transmission design for irs-aided secure cognitive radio systems against internal eavesdropping," *IEEE Transactions on Wireless Communications*, vol. 23, no. 12, pp. 17 841–17 855, 2024.

[12] C. Pan, G. Zhou, K. Zhi, S. Hong, T. Wu, Y. Pan, H. Ren, M. D. Renzo, A. Lee Swindlehurst, R. Zhang, and Zhang, "An overview of signal processing techniques for ris/irs-aided wireless systems," *IEEE Journal of Selected Topics in Signal Processing*, vol. 16, no. 5, pp. 883–917, 2022.

[13] S. Hu, Z. Wei, Y. Cai, C. Liu, D. W. K. Ng, and J. Yuan, "Robust and secure sum-rate maximization for multiuser miso downlink systems with self-sustainable irs," *IEEE Transactions on Communications*, vol. 69, no. 10, pp. 7032–7049, 2021.

[14] W. U. Khan, E. Lagunas, A. Mahmood, S. Chatzinotas, and B. Ottersten, "Ris-assisted energy-efficient leo satellite communications with noma," *IEEE Transactions on Green Communications and Networking*, vol. 8, no. 2, pp. 780–790, 2024.